Orbital
The electronic journal of chemistry

the electronic journal of chemistry

Full Paper | http://dx.doi.org/10.17807/orbital.v16i3.19016

Novel Piperidone Hydrazine Carbodithioate Derivative: Synthesis, *In Silico* Drug-Likeness Analysis and Anticancer Properties

Athavan Alias Anand Selvam*

An efficient synthesis of a novel compound of hydrazine carbodithioate derivative of piperidone, (*E*)-methyl-2-(3-methyl-2,6-diphenylpiperidin-4-ylidene)hydrazinecarbodithioate (**1**), was performed using methyl dithiocarbazinate and 3-methyl-2,6-diphenylpiperidin-4-one as the starting materials. The reaction was carried out in an acidic medium using methanol as a solvent. The novel compound was characterized by FTIR, Mass, and NMR spectral techniques. The hydrazine carbodithioate derivative (**1**) was then tested for its anticancer activity against the liver cancer cell line, Hep G2, using the MTT assay. The IC_{50} values of the newly synthesized compound were found to be 34.33 ± 0.79 µM (24 hours) and 27.64 ± 1.42 µM (48 hours). The *in vitro* antitumor studies demonstrated that the novel compound (**1**) exhibited good inhibitory activity against the Hep G2 cancer cells. Furthermore, *in silico* properties such as lipophilicity, water solubility, pharmacokinetic properties, drug likeness, and medicinal chemistry were analyzed using the SwissADME tool.

Graphical abstract

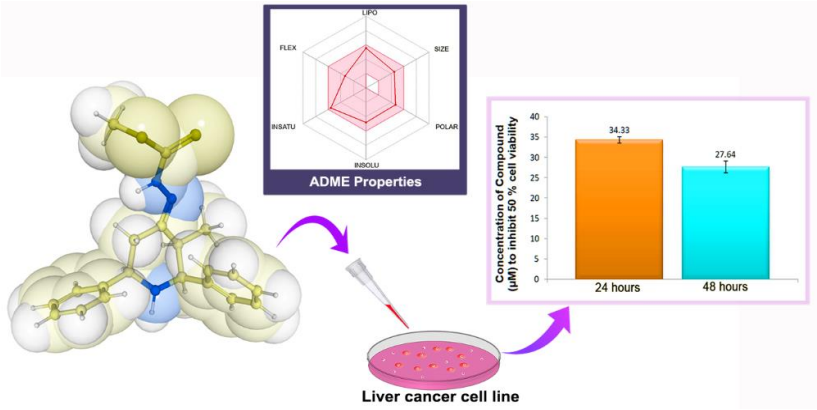

Keywords

Anticancer
Drug likeness
Hep G2 cell lines
Hydrazine carbodithioate
Piperidone
SwissADME

Article history

Received 06 Jul 2023
Revised 06 Jun 2024
Accepted 29 Jul 2024
Available online 27 Sep 2024

Handling Editor: Adilson Beatriz

1. Introduction

Liver cancer was one of the most dominant cancers and highly lethal among both men and women for decades in most countries. However, liver cancer mortality stabilized since 2013 among males and since 2014 among females after years of increasing rates. According to reports, liver cancer was the fourth most common cancer death among American Indian/Alaska Native (AI/AN) and Hispanic males and second among Asian/Pacific Islander (API) males. Death rates increased among AI/AN male, remained stable among White and Hispanic males, and decreased among Black and API males. Liver cancer death rates were then stable in males and females after a period of increasing rates [1]. According to the

Department of Chemistry, Prayoga Institute of Education Research, Bengaluru, Karnataka, Pin code 560116, India. *Corresponding author. E-mail: **athavan@prayoga.org.in**

GLOBOCAN 2020 estimation, over 905677 new cases and 830180 died from liver cancer and this makes liver cancer the second leading cause of cancer death in males and the sixth in females across the world [2]. Research studies indicate that the deregulated mammalian target of Rapamycin (mTOR) signalling significantly contributes to the primary liver cancers such as hepatocellular carcinoma (HCC) and intrahepatic cholangiocarcinoma (iCCA) [3]. Recent advancements in synthetic organic chemistry and biomedical engineering allow the discovery of potent small molecule drugs against liver cancer. Heterocyclic compounds containing sulphur and nitrogen drawn considerable attention due to their pharmacological activities [4,5,6]. Compounds such as Sorafenib tosylate, Cabozantinib and Regorafenib were studied for antitumor effects of the hepatocellular carcinoma and their mechanisms of action based on molecular profiling [7,8,9].

Among heterocycles, the derivatives of piperidin-4-one have been widely explored for their significant biological activities [10,11,12] especially modified 2,6-diarylpiperidin-4-one derivatives. Several substituted 2,6-diarylpiperidin-4-ones were showed variety of drug-like properties such as antiproliferative [13], anticancer [14,15,16], antituberculosis [17], analgesic-antipyretic [18], antibacterial and antifungal [19]. On the other hand, organosulphur compounds also played a remarkable role in small molecule drug discovery [20,21]. Several pieces of the research reported that the naturally occurring sulphur compounds present in food items acted as nutraceuticals [22] and were good in preventing human cancer [23], cardiovascular diseases [24], and blood clots [25]. Laboratory synthesized organo-sulphur compounds such as hydrazine carbodithioate also showed biological activities such as antifilarial [26], anti-HIV [27], antimicrobial and anticancer [28]. From the above facts, a novel hydrazine carbodithioate derivative of 2,6-diarylpiperidin-4-one was synthesized and studied for its *in silico* drug likeness and *in vitro* anticancer properties. The molecular structure of the newly synthesized compound was elucidated using spectral techniques. The *in silico* studies was carried out for the new compound **1** using SwissADME online tool to analyse its physiochemical properties, lipophilicity, water solubility, pharmacokinetics, drug likeness and medicinal chemistry properties. In order to investigate the anticancer properties of the novel sulphur containing scaffold, the compound (**1**) was tested against the liver cancer cell line, Hep G2 using 3-(4,5-dimethylthiazol-2-yl)-2,5-diphenyltetrazolium bromide (MTT) assay.

2. Material and Methods

2.1 Instrumentation and General Techniques

The melting point was determined in an open capillary tube and is uncorrected. Infrared spectrum was recorded on Thermo Nicolet FT–IR model iS5 spectrophotometer using KBr pellet. The NMR spectra were recorded at 400 MHz Bruker instruments using Tetramethylsilane (TMS) as an internal standard. Deuterated chloroform was used to record NMR spectra and the chemical shifts are reported in δ units (parts per million) relative to the standard. Mass spectrum was recorded on Thermo Nicolet Exactive Plus mass spectrometer. All reactions were monitored by thin-layer chromatography using silica gel pre-coated aluminium sheets of Merck TLC 60 F254 and visualized in a UV light chamber. All reactions were carried out using analytical grade solvents without further purification.

2.2 Synthetic Procedures

2.2.1 Preparation of Methyl Dithiocarbazinate (Ib)

To the cold mixture of potassium hydroxide (0.084 g, 1.5 mmol.), absolute ethanol (10 mL), and hydrazine hydrate (0.048 g, 1.5 mmol.), carbon disulfide (0.114 g, 1.5 mmol.) was added dropwise while maintaining the temperature at 5 °C. The potassium salt of dithiocarbazinate formed was methylated with ice-cooled iodomethane (0.234 g, 1.65 mmol.) at <5 °C and the reaction mixture was allowed to stir for an additional 90 minutes. The white precipitate formed was collected and recrystallized from chloroform [29].

2.2.2 Preparation of 3-methyl-2,6-diphenylpiperidin-4-one (IIa)

The compound **IIa** was synthesized by Mannich condensation of aromatic aldehyde, ketone and ammonium acetate in ethanol. A mixture of benzaldehyde (0.212 g, 2.0 mmol), butanone (0.072 g, 1.0 mmol) and ammonium acetate (0.077 g, 1.0 mmol) in ethanol (30 mL) was heated at 60 °C for 5 minutes. The mixture was kept at room temperature for 12 hours. Diethyl ether (40 mL) was added followed by concentrated hydrochloric acid (25 mL) and cooled in ice water. The hydrochloride salt precipitated was filtered and washed with ethanol:ether (1:5, 20 mL) mixture. The washed salt was suspended in acetone (10 mL) and the liquid ammonia (5 mL) was added dropwise to make it alkaline. The precipitate formed on dilution with distilled water was filtered, dried and recrystallized from absolute ethanol [30,31].

2.2.3 Procedure for the synthesis of the compound 1

In a 100 mL RB flask, compound **IIa** (0.265 g, 1.0 mmol) was dissolved in methanol (20 mL). Methyl dithiocarbazinate **Ib** (0.122 g, 1.0 mmol) and concentrated hydrochloric acid (0.2 mL) were added to the reaction mixture and allowed it to reflux for 2 hours. The completion of reaction was confirmed by thin-layer chromatography and the reaction mixture was cooled to room temperature. The solid separated was filtered and the crude product was recrystallized from methanol. The spectral data of compound **1** were given below

(*E*)-methyl-2-(3-methyl-2,6-diphenylpiperidin-4-ylidene)hydrazinecarbodithioate: Chemical Formula: $C_{20}H_{23}N_3S_2$; White powder; Yield: 0.288 g, 78%; mp: 172–174 °C; FTIR (KBr) (vmax, cm^{-1}): 3295, 3440 (NH), 2871, 2928, 2963 (aliphatic C-H), 1533 (C=N), 1492, 1480 (C=S); ^{1}H NMR (400 MHz, $CDCl_3$, δ ppm): 0.95 (d, 3H, H3'a), 2.58 (s, 3H, H7), 2.03 (s, 1H, H3a), 2.25 (t, 1H, H5a), 3.55 (d, 1H, H2a), 3.87 (d, 1H, H6a), 2.93 (d, 1H, H5e), 7.24-7.45 (m, 10H, Aromatic-H), 10.15 (s, 1H, NH); ^{13}C NMR (125 MHz, $CDCl_3$): δ 12.0 (CH_3, C-3'), 17.7 (CH_3, C-7), 36.2 (CH_2, C-5), 45.6 (CH, C-3), 60.9 (CH, C-6), 69.1 (CH, C-2), 126.7-128.7 (Aromatic carbons), 157.4 (C=N, C-4), 142.2, 142.6 (*ipso* carbons), 201.6 (C=S, C-8); HRMS (M+Na): 392.1233.

2.3 *In Silico* ADME studies

The SwissADME web tool was used to predict the drug likeness of compound **1**. The tool was freely accessible at **http://www.swissadme.ch** and meant for user-friendly submission and easy analysis of the results, also for non-experts in CADD (Computer Aided Drug Design). In comparison to the state-of-the-art free web-based tools for ADME and pharmacokinetics, and in addition to having exclusive access to expert methods, this CADD tool was developed by the Molecular Modeling Group of the SIB, Swiss

Institute of Bioinformatics. In this study, the novel compound (**1**) was subjected to *in silico* ADME (Absorption, Distribution, Metabolism and Excretion) prediction for the following properties [32].

2.3.1 Physicochemical properties

SwissADME's physicochemical properties section offered a range of predictions for molecular properties that impact the pharmacokinetics and pharmacodynamics of small molecules. These predictions included key properties such as molecular weight, logP (lipophilicity), number of atomic heavy atoms, hydrogen bond donors and acceptors, refractivity, fraction Csp3, TPSA (topological polar surface area), and number of rotable bonds. These predictions were widely accepted as useful descriptors in various models and rules for quick estimating of important ADME properties such as absorption and brain access.

2.3.2 Lipophilicity

The lipophilicity of compounds was found to affect their ability to cross biological barriers and access certain targets. Compounds with high lipophilicity were observed to have better membrane permeability and were able to cross biological barriers more easily, but they were also more prone to non-specific binding and accumulation in lipid-rich tissues. In contrast, compounds with low lipophilicity were found to have lower bioavailability and limited access to certain targets, but were less likely to cause off-target effects or toxicity. The Swiss ADME platform provided access to five predictive models that were freely available, including XLOGP3, which was an atomistic method that used corrective factors; WLOGP, which was a purely atomistic method based on the fragmental system; MLOGP, which was a topological method dependent on a linear relationship that was implemented with 13 molecular descriptors; SILICOS-IT, which was a hybrid method dependent on 27 fragments and 7 topological descriptors; and iLOGP, which was a physics-based method that used the Generalized-Born and solvent accessible surface area (GB/SA) model to calculate free energies of solvation in n-octanol and water. The platform also provided the consensus *log* $P_{o/w}$ value, which was the average of the predicted values from all five methods.

2.3.3 Water Solubility

Water solubility was considered an important property in drug discovery because it influenced the bioavailability and pharmacokinetic properties of a compound. In SwissADME, water solubility was predicted using three models: (i) the ESOL (Estimated SOLubility) model, (ii) a model from Ali et al., and (iii) SILICOS-IT, a machine learning-based approach. These models were trained on a large dataset of experimentally measured solubility values. All predicted values were the decimal logarithm of the molar solubility in water (log S). SwissADME also provided solubility in mol/L and mg/mL, along with qualitative solubility classes.

2.3.4 Pharmacokinetics

In the pharmacokinetics section, the particular ADME properties of the organic compound under investigation were evaluated. The predictions for passive human gastrointestinal absorption (HIA) and blood-brain barrier (BBB) permeation both consisted of the readout of the BOILED-Egg model, an intuitive graphical classification mode. The information of compounds was substrate or non-substrate of the permeability glycoprotein (P-gp) was key to appraise active efflux through biological membranes, for instance from the gastrointestinal wall to the lumen or from the brain. In this prediction, five major inhibitors (CYP1A2, CYP2C19, CYP2C9, CYP2D6, CYP3A4) and Log Kp (skin penetration coefficient) were studied. These models were estimated to be important ADME behaviours and were of great support for pharmacokinetics optimization and evaluation of small drug-like organic compounds.

2.3.5 Druglikeness

The druglikeness of the organic compounds was predicted based on five rule-based filters namely, Lipinski, Ghose, Veber, Egan, and Muegge [33]. The rules are defined as,

(i) Lipinski's rule includes molecular weight ≤ 500, MLOGP (lipophilicity) ≤ 4.15, hydrogen bond acceptors ≤ 10 and hydrogen bond donors ≤ 5.

(ii) Ghose's rule includes 160 ≤ molecular weight ≤ 480, −0.4 ≤ WLOGP (lipophilicity) ≤ 5.6, 40 ≤ the molar refractivity ≤ 130 and 20 ≤ number of atoms ≤ 70.

(iii) Veber's rule includes the number of rotatable bonds ≤ 10 and the total polar surface area ≤ 140.

(iv) Egan's rule includes WLOGP (Lipophilicity) ≤ 5.88 and the total polar surface area ≤ 131.6.

(v) Muegge's rule includes 200 ≤ molecular weight ≤ 600, −2 ≤ XLOGP3 (lipophilicity) ≤ 5, the total polar surface area ≤ 150, the number of rings ≤ 7, the number of carbons > 4, the number of heteroatoms > 1, the number of rotatable bonds ≤ 15, the hydrogen bond acceptors ≤ 10 and the hydrogen bond donors ≤ 5.

2.3.6 Medicinal Chemistry

The purpose of this section is to help medicinal chemists in their daily drug discovery endeavours. This section had included four parameters: (i) PAINS (pan assay interference compounds), which indicated the organic compounds containing substructures showing potent response in assays irrespective of the protein target; (ii) Brenk, information on putatively toxic, chemically reactive, metabolically unstable or that bore properties responsible for poor pharmacokinetics; (iii) Leadlikeness, which indicated properties similar to drug-likeness, focusing on physicochemical boundaries defining a good lead, and (iv) Synthetic accessibility (SA), where the fragmental contributions to SA were summed and corrected by the terms describing size and complexity, such as macrocycles, chiral centres, or spiro functions. This SA score had demonstrated how this simple and fast methodology could help prioritize molecules to synthesize. The important numerical data of *in silico* analysis for compound **1** are tabulated in Table 1 and the detailed data is given in the supplementary material (Table S1).

2.4 *In Vitro* Anticancer Studies

The cytotoxic effect of the synthesized compound **1** on the human hepatoma cell-line, Hep G2, was evaluated through MTT assay as described earlier [34]. Human hepatoma cell-

line, Hep G2, was obtained from the National Centre for Cell Science, Pune, India. The synthesized compound (**1**) was dissolved quantitatively in dimethyl sulfoxide (DMSO, Sigma, USA) and diluted to make the stock solution. Hep G2 cells were seeded at a density of 5×10^3 cells per well into 96-well plates. The cells were treated with compound **1** at various concentrations, *viz.*, 10 µM, 20 µM, 30 µM, 40 µM, 50 µM, 60 µM, 70 µM, 80 µM, 90 µM and 100 µM and incubated for 24 hours and 48 hours, respectively. The cells were then assayed by the addition of 20 µL of MTT (5 mg mL^{-1} in phosphate-buffered saline) per well and incubated in the dark at 37 ºC for 3 hours. The purple formazan crystals formed after 3 hours were dissolved in 100 µL of DMSO after aspirating the MTT and incubated for a further 10 minutes. The mitochondrial dehydrogenase in viable cells that reduces MTT to blue formazan product was measured at 570 nm (measurement) and 630 nm (reference) using a 96-well plate reader (Bio-Rad, Hercules, CA, USA). Data were collected from six independent experiments and used to calculate the respective means. The percentage of inhibition was calculated from the data using the following formula:

[(Mean absorbance of treated cells) / (Mean absorbance of sham control cells) × 100]

Table 1. The *in silico* ADME prediction results for compound **1** using SwissADME tool.

Physiochemical Properties		
1	Formula	$C_{20}H_{23}N_3S_2$
2	Molecular Weight	369.55
3	Number of heavy atoms	25
4	Number of aromatic heavy atoms	12
5	Number of rotatable bonds	5
6	Number of H-bond acceptors	2
7	Number of H-bond donors	2
8	Topological polar surface area	93.81
Lipophilicity		
9	Consensus Log $P_{o/w}$	3.92
Water Solubility		
10	Silicos-IT LogSw	-6.73
Pharmacokinetics		
11	GI absorption	High
12	BBB permeant	No
13	CYP1A2 inhibitor	Yes
14	CYP2C19 inhibitor	Yes
15	CYP2C9 inhibitor	Yes
16	CYP3A4 inhibitor	Yes
Druglikeness		
17	Lipinski number of violations	0
18	Ghose number of violations	0
19	Veber number of violations	0
20	Egan number of violations	0
21	Muegge number of violations	0

3. Results and Discussion

The derivatives of piperidin-4-ones are of considerable interest because of their diverse biological activities such as anticonvulsant, antioxidant, anticancer, analgesic and so on [35,36,37]. Several multicomponent reaction procedures were reported to synthesis piperidin-4-one derivatives [38]. In this study, 3-methyl-2,6-diphenylpiperidin-4-one (**IIa**) was synthesized by Mannich condensation with butanone, benzaldehyde, and ammonium acetate in 1:2:1 ratio in ethanol. The compound methyl dithiocarbazinate (**Ib**) was obtained by reacting hydrazine hydrate with carbon disulfide in the presence of potassium hydroxide and the dithiocarbazinate salt (**Ia**) formed was methylated with methyl iodide at lower temperature. The title compound (**1**) was synthesized in good yields by refluxing 3-methyl-2,6-diphenylpiperidin-4-one (**IIa**) and methyl dithiocarbazinate (**Ib**) in methanol in the presence of the catalytic amount of concentrated hydrochloric acid (Scheme 1).

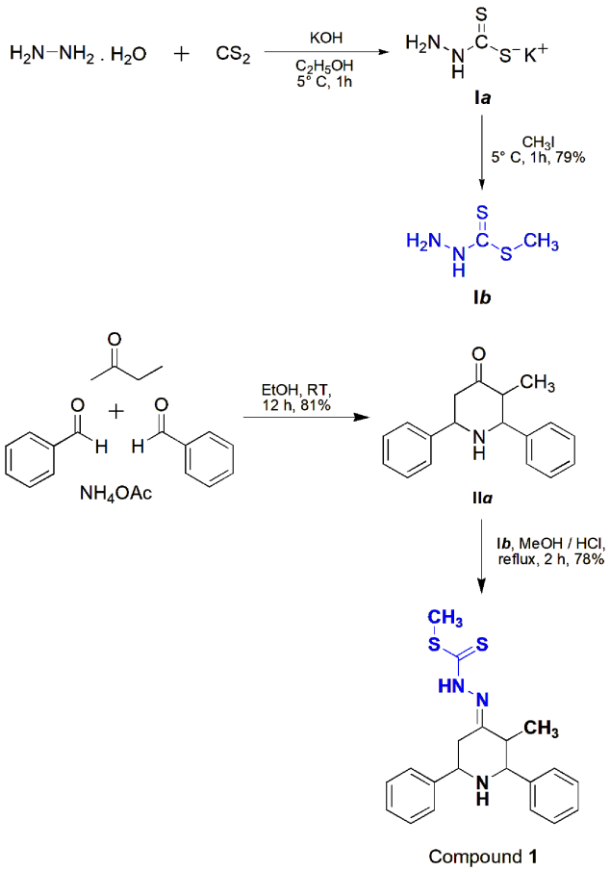

Scheme 1 Synthesis of novel hydrazine carbodithioate derivative (**1**) of piperidone

3.1 FT-IR and Mass spectral analyses of compound 1

In the FT-IR spectrum of compound **1**, (Figure S1 in the Supplemental Materials) the bands appeared in the region of 3295 cm^{-1} and 3440 cm^{-1} owing to the –NH- groups of the compounds. The absorptions in the region 2871-2963 cm^{-1} are due to the aliphatic and the aromatic CH stretching of compound **1**. The C=N stretching of the compound was confirmed by the presence of a sharp band observed in the region 1533 cm^{-1}. The sharp band at 1492 cm^{-1} and 1480 cm^{-1} correspond to the C=S and C-S stretching respectively. The presence of C=N, C=S stretching bands and the absence of carbonyl group band around 1700 cm^{-1} confirmed the formation of the targeted compound. Mass spectrum (Figure S2) of compound **1** shows a peak at 392.1233 which confirmed the product formation and its purity.

3.2 ^{1}H and ^{13}C NMR spectral analyses of compound 1

The numbering pattern followed for compound **1** to explain NMR spectra is given in figure 1. The ^{1}H NMR spectrum of compound **1**, (Figures S3 and S4 in the Supplemental Materials) showed a doublet at 0.95 ppm with three protons integral is assigned to methyl group protons at C3 of the piperidone ring. Similarly, the presence of S-CH_3 methyl protons was confirmed by a singlet at 2.58 ppm with

three protons integral. The H-3a proton resonated as a broad singlet at 2.03 ppm with one proton integral. The triplet appeared at 2.25 ppm with one proton integral assigned to H-5a proton. The peaks for two benzylic protons H-2a and H-6a appeared at 3.55 ppm and 3.87 ppm as doublets with one proton integral each. The doublet at 2.93 ppm is corresponding to the equatorial proton H-5e. The phenyl protons of compound **1** are resonated at the aromatic region of the spectrum 7.24-7.45 ppm and the sharp singlet that appeared in the deshielded region at 10.15 ppm is assigned to the –NH proton of piperidyl ring.

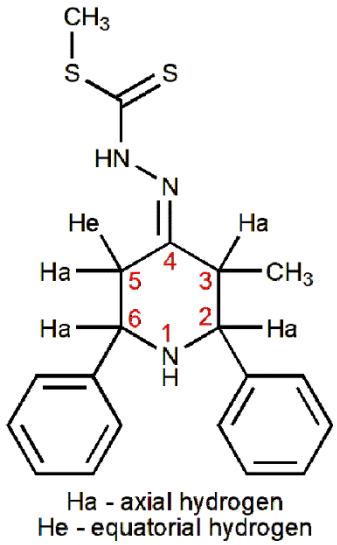

Fig. 1. Numbering pattern of compound **1** followed for the spectral explanations.

In the ^{13}C NMR of compound **1**, (Figure S5 in the Supplemental Materials) the signal obtained at 12.0 ppm is assigned to methyl group carbon at C3 of the piperidone ring. The signal for S-CH_3 methyl carbon is observed at 17.7 ppm. The signals 36.2, 45.6, 60.9 and 69.1 ppm appeared in the aliphatic regions are assigned for C5, C3, C6 and C2 carbons respectively. The signals of phenyl carbons attached to the piperidyl ring were observed at 126.7-128.7 ppm whereas the C4 carbon signal appeared at 157.4 ppm. The two signals at 142.2 and 142.6 ppm observed due to *ipso* carbons. The deshielded region signal at 201.6 ppm is assigned for C=S carbon of compound **1**.

3.3 *In Silico* Studies

The *in silico* drug likeness properties of the novel compound were analysed using SwissADME online tool. Swiss ADME is an online tool of Swiss institute of bioinformatics was used to identify particular ADME behaviours of the synthesized compound (**1**). The predictions and analysis were based on the numerical data obtained under the headings (i) physiochemical properties, (ii) lipophilicity, (iii) water solubility, (iv) pharmacokinetics and (v) medicinal chemistry. The drug likeness of compound **1** was evaluated using SwissADME web tool. The results included a bioavailability radar which represents six physicochemical properties: (i) Lipophilicity (XLOGP3 between −0.7 and +5.0), (ii) size (molecular weight between 150 and 500 g/mol), (iii) polarity (the total polar surface area between 20 and 130 $Å^2$), (iv) solubility (log S not higher than 6), (v) saturation (fraction Csp3 not less than 0.25), and (vi) flexibility (the number of rotatable bonds not more than 9). The bioavailability radar of compound **1** and upon interaction for six physicochemical properties was shown in Figure 2a. The efficiency of the BOILED-Egg method in predicting human blood-brain barrier (BBB) penetration and gastrointestinal absorption was also demonstrated. The BOILED-Egg representation of compound **1** created by SwissADME is displayed in Figure 2b. This method is based on the compound's lipophilicity (WLOGP) and polarity (topological polar surface area, TPSA). Molecules located in the yellow region (BOILED-Egg's yolk) were predicted to permeate the BBB passively, while those in the white region (BOILED Egg's white) were predicted to be passively absorbed by the gastrointestinal tract. Blue (PGP+) and red (PGP-) dots indicated organic compounds that were predicted to be effluxed and not effluxed from the central nervous system by P-glycoprotein, respectively.

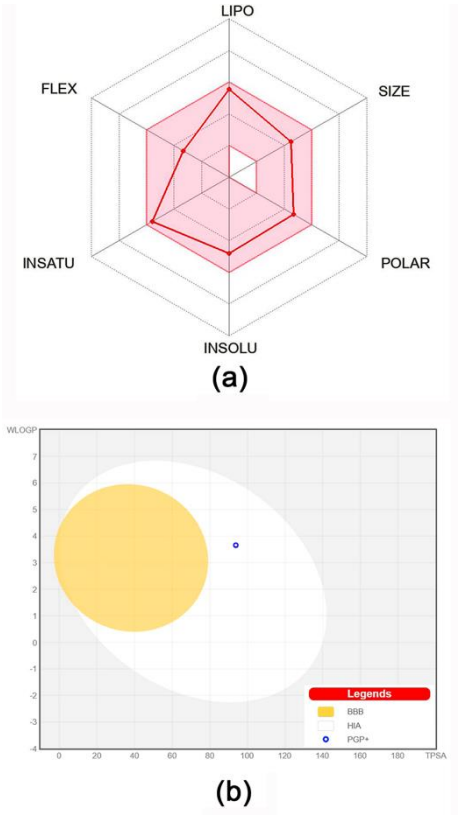

Fig. 2. (a) The Bioavailability Radar of compound **1** from SwissADME web portal; (b) The BOILED-Egg method of representation showed the position of compound **1** in the WLOGP-versus-TPSA graph.

In the bioavailability radar (Figure 2a), the pink area represented the optimal range of these properties, and the red line represented the properties of the compounds. The bioavailability radar figure showed that the red lines of the synthesized compound (**1**) were in the range of the pink area. Therefore, it was concluded that compound **1** was predicted orally as bioavailable. According to the BOILED-Egg prediction generated by SwissADME for compound **1** (Figure 2b), the molecule was located in the white region with a blue point. This indicated that the compound **1** was likely to be absorbed by the gastrointestinal tract and unable to pass through the BBB. Additionally, the blue point signified that the compound was PGP+, and effluxes from the central nervous system by the P-glycoprotein.

Using the Silicos IT LogSw descriptor of SwissADME, the water solubility of compound **1** was predicted and its LogSw values were determined to be −6.73. According to the

SwissADME LogSw scale, compounds with values less than (more negative than) −6 were classified as poorly soluble. The assessment of lipophilicity was conducted through the prediction of the logarithm of the n-octanol/water partition coefficient using the Consensus $LogP_{o/w}$ descriptor of SwissADME. To achieve good oral bioavailability, which entails good permeability and solubility, a moderate logP value between 0 and 3 was recommended [39]. The predicted value of $LogP_{o/w}$ for compound **1** was 3.92. SwissADME was employed to estimate the metabolism of the synthesized compound by inhibiting the principal cytochromes (CYP) of the P450 superfamily, including CYP1A2, CYP2C19, CYP2C9, CYP2D6, and CYP3A4. CYP enzyme inhibition, a primary mechanism for drug–drug interactions based on metabolism, involved competition with other drugs for the same enzyme binding site. The inhibition of enzymes impairs the biotransformation or clearance of clinically used drugs, including several anticancer agents, leading to elevated plasma levels of drugs that affect the therapeutic outcome. In the case of a prodrug, the effect is reduced. Therefore, the inhibition of CYPs resulted in drug toxicity or lack of efficacy [40]. CYP2C19 was responsible for metabolizing several drugs and plays a role in the detoxification of potential carcinogens or bioactivation of some environmental procarcinogens [41]. Drugs with a narrow therapeutic index were primarily metabolized by CYP2C9 [42]. CYP2D6 was highly polymorphic, and its metabolism varies; individuals with reduced or no activity of this enzyme were at risk of reduced drug efficacy or adverse effects [43]. The predicted outcomes suggested that compound **1** was likely to inhibit CYP1A2, CYP2C19, CYP2C9, and CYP3A4, but not CYP2D6. Finally, compound **1** underwent drug-likeness prediction using five different rule-based filters, namely Lipinski, Ghose, Veber, Egan, and Muegge. The evaluation showed that the compound complied with all rules and did not violate any of them, indicating good drug-likeness.

3.4 *In Vitro* Biological Studies

The anticancer activities of the compound **1** were evaluated against liver cancer cell lines, Hep G2 through MTT assay. The minimum concentrations of the compound **1** that inhibited 50% of cell growth (IC_{50}) in µM were calculated. The inhibitory effects of the novel compound **1** on Hep G2 cell line after 24 hours and 48 hours are shown in Figure 3. Compound **1** showed a good inhibition of cell viability against Hep G2 cell lines, obtaining IC_{50} values (µM) 34.33 ± 0.79 for 24 hours, and 27.64 ± 1.42 for 48 hours respectively.

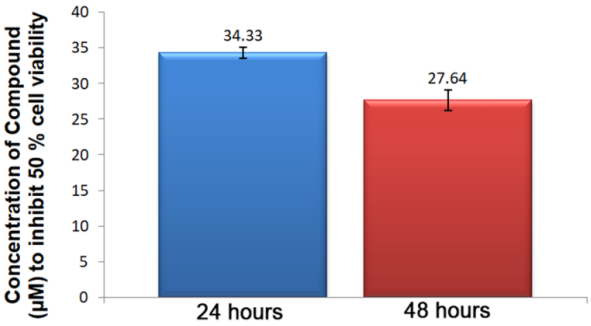

Fig. 3. IC_{50} range of compound **1** against human liver cancer cell line, Hep G2. Data shown are the mean values from six independent experiments.

The anticancer studies clearly indicated that the hydrazine carbodithioate derivatives (**1**) of piperidone inhibited cell viability against liver cancer cell lines at micromolar concentrations. The carbodithioate and piperidone scaffolds play an important role in inhibiting the tested cell line, Hep G2. The results showed that the compound (**1**) exhibited significant inhibition against liver cancer cell line with IC_{50} values 34.33 ± 0.79 for 24 hours, and 27.64 ± 1.42 for 48 hours respectively. The anticancer studies revealed that the hydrazine carbodithioate derivative of piperidone (**1**) with organosulphur atoms, piperidone scaffold and aromatic phenyl rings showed inhibitory activities against Hep G2 cell line.

4. Conclusions

In conclusion, a convenient and effective method was reported to synthesize hydrazine carbodithioate derivative (**1**) of piperidone with good yield. The absorption peaks obtained from FTIR spectrum, mass spectrum and the chemical shifts obtained from NMR spectra confirmed the structure of the novel compound. The *in silico* ADME studies of the novel piperidone derivative using SwissADME tool was predicted orally as bioavailable. The compound was likely absorbed by the gastrointestinal and not permeated through the BBB. The *in silico* scores obtained for physiochemical properties, lipophilicity, water solubility, and pharmacokinetics supported the drug-likeness of the newly synthesized compound. Furthermore, in the evaluation of anticancer studies, compounds **1** exhibited significant inhibition against Hep G2 cancer cell line with IC_{50} values 34.33 ± 0.79 for 24 hours, and 27.64 ± 1.42 for 48 hours respectively. In summary, the newly synthesized hydrazine carbodithioate derivative of piperidone demonstrated promising *in silico* ADME and anticancer properties, highlighting its potential as a lead compound for further drug development.

Supporting Information

Spectra images and the *in silico* results of compound **1** (.doc).

References and Notes

[1] Cronin, K. A.; Scott, S.; Firth, A. U.; Sung, H.; Henley, S. J.; Sherman, R. L.; Siegel, R. L.; Anderson, R. N.; Kohler, B. A.; Benard, V. B.; Negoita, S.; Wiggins, C.; Cance, W. G.; Jemal, A. *Cancer* **2022**, *128*, 4251. [Crossref]

[2] Sung, H.; Ferlay, J.; Siegel, R. L.; Laversanne, M.; Soerjomataram, I.; Jemal, A.; Bray, F. *CA Cancer J. Clin.* **2021**, *71*, 209. [Crossref]

[3] Lu, X.; Paliogiannis, P.; Calvisi, D. F.; Chen, X. *Hepatology* **2021**, *73*, 49. [Crossref]

[4] Sarkı, G.; Tüzün, B.; Ünlüer, D.; Kantekin, H. *Inorganica Chim Acta* **2023**, *545*, 121113. [Crossref]

[5] Saravanan, K.; Elancheran, R.; Divakar, S.; Anand, S. A. A.; Ramanathan, M.; Kotoky, J.; Lokanath, N. K.; Kabilan, S. *Bioorg Med Chem Lett.* **2017**, *27*, 1199. [Crossref]

[6] Bhat, M.; Poojary, B.; Kalal, B. S.; Swamy, P. M. G.; Kabilan, S.; Kumar, V.; Shruthi, N.; Anand, S. A. A.; Pai, V. R. *Future Med. Chem.* **2018**, *10*, 1017. [Crossref]

[7] Kissel, M.; Berndt, S.; Fiebig, L.; Kling, S.; Ji, Q.; Gu, Q.; Lang, T.; Hafner, F.; Teufel, M.; Zopf, D. *Oncotarget*

2017, *8*, 107096. [Crossref]

[8] Liu, S.; Du, Y.; Ma, H.; Liang, Q.; Zhu, X.; Tian, J. *Cancer Lett.* **2019**, *453*, 74. [Crossref]

[9] Deng, S.; Solinas, A.; Calvisi, D. F. *Future Oncol.* **2021**, *11*, 756672. [Crossref]

[10] Smith, R. B.; Roberts, W.; Upenieks, M.; Gibson, M. Z.; Wentzel, M. T.; Grice, K. A.; Zingales, S. K. *Heterocyclic Communications* **2023**, *29*, 20220162. [Crossref]

[11] Anchoori, R. K.; Tan, M.; Tseng, S. H.; Peng, S.; Soong, R. S.; Algethami, A.; Foran, P.; Das, S.; Wang, C.; Wang, T. L.; Liang, H.; Hung, C. F.; Roden, R. B. S. *PLoS One* **2020**, *15*, e0227727. [Crossref]

[12] Li, N.; Bai, X.; Zhang, L.; Hou, Y. *Acta Crystallogr. C Struct. Chem.* **2018**, *74*, 1171. [Crossref]

[13] Aeluri, R.; Alla, M.; Bommena, V. R.; Murthy, R.; Jain, N. *Asian J. Org. Chem.* **2012**, *1*, 71. [Crossref]

[14] Anand, S. A. A.; Loganathan, C.; Thomas, N. S.; Saravanan, K.; Alphonsa, A. T.; Kabilan, S. *New J. Chem.* **2015**, *39*, 7120. [Crossref]

[15] Anand, S. A. A.; Loganathan, C.; Thomas, N. S.; Saravanan, K.; Alphonsa, A. T.; Kabilan, S. *Phosphorus Sulfur Silicon Relat. Elem.* **2016**, *191*, 1396. [Crossref]

[16] Anand, S. A. A.; Loganathan, C.; Saravanan, K.; Kabilan, S. *Int. Lett. Chem. Phy. Astron.* **2015**, *60*, 161. [Crossref]

[17] Aridoss, G.; Amirthaganesan, S.; Kim, M.S.; Kim, Y. T. J.; Jeong, Y.T. *Eur. J. Med. Chem.* **2009**, *44*, 4199. [Crossref]

[18] Tripathi, P.; Tripathi, A.C.; Chawla, V.; Saraf, S.K. *Eur. J. Med. Chem.* **2014**, *82*, 439. [Crossref]

[19] Balasubramanian, S.; Ramalingan, C.; Aridoss, G.; Kabilan, S. *Eur. J. Med. Chem.* **2005**, *40*, 694. [Crossref]

[20] Štefanová, I.; Bittnerová, P.; Zápal, J.; Kuzma, M.; Kubec, R. *J. Agric. Food Chem.* **2023**, *71*, 5712. [Crossref]

[21] Anand, S.A.A.; George, K.; Thomas, N.S.; Kabilan, S. *Phosphorus Sulfur Silicon Relat. Elem.* **2020**, *195*, 821. [Crossref]

[22] Goncharov, N. V.; Belinskaia, D. A.; Ukolov, A. I.; Jenkins, R. O.; Avdonin, P. V. In: Nutraceuticals, 2nd Ed. Efficacy, Safety and Toxicity. Gupta, R. C.; Lall, R.; Srivastava, A., eds. Academic Press: Cambridge, 2021, p. 911-924.

[23] Bommareddy, A.; VanWert, A. L.; McCune, D. F.; Brozena, S. L.; Witczak, Z.; Singh, S. V. In: Critical Dietary Factors in Cancer Chemoprevention. Ullah, M.; Ahmad, A., eds. Springer: New York, 2016.

[24] Vazquez-Prieto, M. A.; Miatello, R. M. *Mol. Aspects Med.* **2010**, *31*, 540. [Crossref]

[25] Block, E.; Bechand, B.; Gundala, S.; Vattekkatte, A.; Wang, K.; Mousa, S. S.; Godugu, K.; Yalcin, M.; Mousa, S. A. *Molecules* **2017**, *22*, 2081. [Crossref]

[26] Klayman, D. L.; Lin, A. J.; McCall, J. W.; Wang, S. Y.; Townson, S.; Grögl, M.; Kinnamon, K. E. *J. Med. Chem.* **1991**, *34*, 1422. [Crossref]

[27] Mahapatra, M.; Kulandaivelu, U.; Saiko, P.; Graser, G.; Szekeres, T.; Andrei, G.; Snoeck, R.; Balzarini, J.; Jayaprakash, V. *Chem. Pap.* **2013**, *67*, 650. [Crossref]

[28] Kulandaivelu, U.; Padmini, V. G.; Suneetha, K.; Shireesha, B.; Vidyasagar, J. V.; Rao, T. R.; Jayaveera, K. N.; Basu, A.; Jayaprakash, V. *Arch. Pharm.* **2011**, *344*, 84. [Crossref]

[29] Klayman, D. L.; Bartosevich, J. F.; Griffin, T. S.; Mason, C. J.; Scovill, J. P. *J. Med. Chem.* **1979**, *22*, 855. [Crossref]

[30] Alphonsa, A. T.; Loganathan, C.; Anand, S. A. A.; Kabilan, S. *J. Mol. Struct.* **2015**, *1100*, 137. [Crossref]

[31] Alphonsa, A. T.; Loganathan, C.; Anand, S. A. A.; Kabilan, S. *J. Mol. Struct.* **2016**, *1106*, 277. [Crossref]

[32] Daina, A.; Michielin, O.; Zoete, V. *Sci. Rep.* **2017**, *7*, 42717. [Crossref]

[33] Parlak, C.; Alver, Ö.; Ouma, C. N. M.; Rhyman, L.; Ramasami, P. *Chem. Pap.* **2022**, *76*, 1471. [Crossref]

[34] Mosmann, T. *J. Immunol. Methods* **1983**, *65*, 55. [Crossref]

[35] Fathima, A.; Kumaravel, V.; Jonathan, D. R.; Sadasivam, S. K.; Yuvashri, R.; Usha, G. *Chem. Phys. Impact.* **2024**, *8*, 100559. [Crossref]

[36] Hu, L.; Ryder, T. R.; Rafferty, M. F.; Feng, M. R.; Lotarski, S. M.; Rock, D. M.; Sinz, M.; Stoehr, S. J.; Taylor, C. P.; Weber, M. L.; Bowersox, S. S.; Miljanich, G. P.; Millerman, E.; Wang, Y.; Szoke, B. G. *J. Med. Chem.* **1999**, *42*, 4239. [Crossref]

[37] Rokkam, S. K.; Mas-Rosario, J. A.; Joshi, B. P.; Joshi, M.; Choudhury, A. R.; Kar, S.; Golakoti, N. R.; Farkas, M. E. *Chem. Biodiversity* **2023**, *20*, e202300822. [Crossref]

[38] Girgis, A. S.; D'Arcy, P.; Aboshouk, D. R.; Bekheit, M. S. *RSC Adv.* **2022**, *12*, 31102. [Crossref]

[39] Zerroug, A.; Belaidi, S.; BenBrahim, I.; Sinha, L.; Chtita, S. *J. King Saud Univ. – Sci.* **2019**, *31*, 595. [Crossref]

[40] Manikandan, P.; Nagini, S. *Curr. Drug Targets* **2018**, *19*, 38. [Crossref]

[41] Wang, Z.; Yang, H.; Wu, Z.; Wang, T.; Li, W.; Tang, Y.; Liu, G. *Chem. Med. Chem.* **2018**, *13*, 2189. [Crossref]

[42] Daly, A. K.; Rettie, A. E.; Fowler, D. M.; Miners, J. O. *J. Pers. Med.* **2018**, *8*, 1. [Crossref]

[43] Tredici, A. L. D.; Malhotra, A.; Dedek, M.; Espin, F.; Roach, D.; Zhu, G. D.; Voland, J.; Moreno, T. A. *Front. Pharmacol.* **2018**, *9*, 305. [Crossref]

How to cite this article

Selvam, A. A. A. *Orbital: Electron. J. Chem.* **2024**, *16*, 154. http://dx.doi.org/10.17807/orbital.v16i3.19016